Dyes and Pigments 92 (2012) 1031–1041

Contents lists available at ScienceDirect

Dyes and Pigments

journal homepage: www.elsevier.com/locate/dyepig

Thermodynamic study of the dimerization equilibrium of methylene blue, methylene green and thiazole orange at various surfactant concentrations and different ionic strengths and in mixed solvents by spectral titration and chemometric analysis

O. Yazdani [a], M. Irandoust [a], Jahan B. Ghasemi [b,*], Sh. Hooshmand [b]

[a] Department of Analytical Chemistry, Faculty of Chemistry, Razi University, Kermanshah, Iran
[b] Department of Chemistry, Faculty of Sciences, K.N. Toosi University of Technology, 41 Kavian Street, Shariati Avenue, Tehran 1541849611, Iran

ARTICLE INFO

Article history:
Received 27 November 2010
Received in revised form
6 July 2011
Accepted 12 July 2011
Available online 26 July 2011

Keywords:
Aggregation
Chemometrics
Methylene blue
Methylene green
Thiazole orange
Critical micelle concentration

ABSTRACT

The monomer–dimer equilibrium and thermodynamics of ionic dyes were investigated by spectrophotometric and chemometric methods. The dimerization constants of methylene blue, methylene green and thiazole orange have been determined by studying the dependence of their absorption spectra at different concentrations of surfactants, ionic strengths and mixed solvents by means of UV–visible spectroscopy in aqueous solutions. The processing of the data, performed for the quantitative analysis of pure spectral profiles, was based on the simultaneous resolution of the overlapping bands in the whole set of absorption spectra. Utilizing the van't Hoff relationship, which describes the dependence of the equilibrium constant on temperature, as a constraint we determined the spectral responses of the monomer and dimer species as well as the enthalpy and entropy of the dimerization equilibrium. The exciton theory was used for the elucidation of the angle between the monomer units and the interaction energy between the molecules of the dimers.

1. Introduction

Aggregation is one of the features of dyes in solution, affecting their colouristic and photo-physical properties and is therefore being of special interest. It is well known that ionic dyes tend to aggregate in diluted solutions, leading to dimer formation, and sometimes even higher order aggregates [1].

Cationic dyes, such as methylene blue (MB) and methylene green (MG) (Fig. 1), are thiazine type dyes, which were initially used for dyeing silk, leather, plastics, paper, and cotton mordanted with tannin, as well as for the production of ink and copying paper in the office supplies industry, and also for the preparation of color lakes. These dyes have also long been used for staining in medicine, bacteriology, and microscopy [2,3]. They can be used as sensitizers in photopolymerization and as a component of a silver free direct-positive color bleaching-out system [4]. Furthermore, the reversible equilibrium between the reduced and oxidized forms of MB and MG, renders these compounds useful as redox indicators [5,6]. MB main uses are related with the determination of glucose, O_2 or ascorbic acid [7,8]. Also previous studies have found that MB molecules existed as a dimer or as aggregates at the surface, as well as a protonated form depending on the concentration and the surface properties [9].

Cyanine dyes are typically based on indole, benzothiazole, benzoxazole and quinoline heterocycles. A widely used intercalating cyanine dye which has an unsymmetrical structure is thiazole orange (TO). Thiazole orange is the oldest synthetic cyanine dyes, today widely used in reticulocyte analysis. The cationic unsymmetrical cyanines such as TO are best known for their fluorogenic behavior in the presence of DNA and RNA [10]. Thiazole orange serves as an ideal scaffold for these conjugates because it is highly fluorescent when bound to DNA. The fluorescence properties of thiazole orange has led to its incorporation into a number of DNA detection or probing systems. This dye was shown to permeate live cell membranes and efficiently stain residual RNA in reticulocytes [11]. In addition, thiazine and cyanine dyes have important photophysical applications [12,13].

The presence of aggregates in the dye solutions may considerably influence their photo-physical behavior. The UV–vis absorption spectroscopy is one of the most suitable methods for quantitative

* Corresponding author. Tel.: +98 21 22850266; fax: +98 21 22853650.
E-mail address: Jahan.ghasemi@gmail.com (J.B. Ghasemi).

0143-7208/$ – see front matter © 2011 Elsevier Ltd. All rights reserved.
doi:10.1016/j.dyepig.2011.07.006

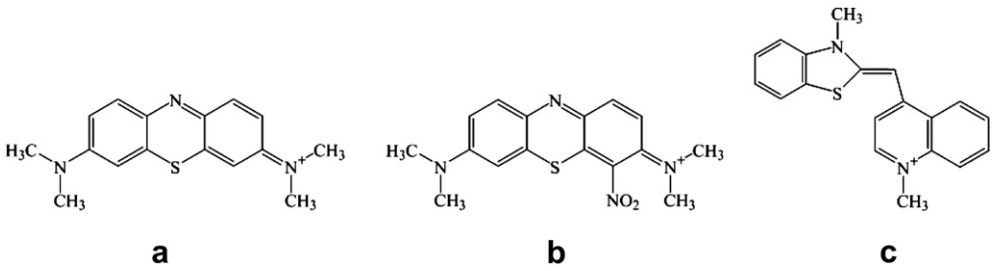

Fig. 1. Dye structures: (a) MB, (b) MG and (c) TO.

study of the aggregation properties of dyes as a function of concentration, since in the concentration range used (10^{-6}–10^{-3} M) monomer-dimer equilibrium mainly exists. In aqueous solution, aggregation can be observed due to the photochemical character of the molecular structure [14,15].

The nature of the self-association of dyes in aqueous solutions, aside from its intrinsic interest, is important in the understanding and interpretation of a great variety of problems, such as dyeing of fibers, tissue staining in biology, spectral change and energy transfer studies, adsorption, and photography. On the other hand, their equilibria can be very useful for analytical application in optical sensors [16].

Thiazine dyes such as MB and MG and also cyanine dyes such as TO, containing polar chromophores are an important group of organic compounds which have a variety of industrial and scientific applications [17]. Therefore, spectroscopic properties of these dyes are still the subject of numerous research studies and controversies [18,19]. Following several authors [20,21], the MB, MG, and TO dimerization equilibrium (Fig. 2), can be expressed a $2(\mathrm{Dye})_{\mathrm{mon}} \rightleftarrows (\mathrm{Dye})_{\mathrm{dim}}$ and the dimer has the form comparable to those depicted in Fig. 2.

In this work, we used some physical constraints to determine the dimeric constants of MB, MG and TO in pure water and some mixed solvents. The information obtained in this study are the monomer and dimer spectra of dyes, their dimerization constant as a function of temperature, effect of different surfactants at various concentrations on the dimerization constants, changes in enthalpy (ΔH) and entropy (ΔS) of the reaction, type of dyes association and effect of additive on structures of aggregations, Data handling was carried out by the DATa ANalysis (DATAN) program.

2. Experimental part

2.1. Material and chemical reagents

All the chemicals used were of analytical reagent grade. Distilled water was used throughout. The investigated dyes (microscopy grade, purity is more than 99%) were purchased from Fluka and Aldrich and were studied without additional purification and their purity was checked spectroscopically. A stock solution of MB (3.0×10^{-4} M), MG (1.0×10^{-3} M) and TO (1.0×10^{-4} M) was prepared by dissolving solid dyes in water. In all experiments the ionic strengths were maintained constant by KCl (Fluka) at 0.5, 1.0 and 1.5 M solutions of the salt. Neutral surfactants, Triton X-100 and Triton X-114 were purchased from Sigma–Aldrich. Cationic surfactants, hexadecyltrimethyl ammonium bromide (HTAB) was obtained from Sigma. The pH of the all solutions was kept constant at 7.0 using Tris buffer.

2.2. Apparatus, instrumentation and software

The absorption spectra were recorded using an Agilent 8453 UV–Vis Diode-Array spectrophotometer, employing Agilent UV–Visible ChemStation software for data acquisition, equipped with a temperature controller and a 1 nm spectral bandpass, and were digitized with five data points per nanometer. Conventional quartz cells (10 mm × 10 mm) and (10 mm × 1 mm) were used throughout. The cuvettes were treated with repel-silane prior to measurements to avoid dye adsorption. The temperature of the cell was kept constant using Hiedolph thermo circulating bath. All absorption spectra were recorded in the wavelength range of 500–750 nm and 350–600 nm for the thiazine and the cyanine dyes, respectively. All calculations were run on a PC with AMD (Athlon 64) as central processing unit (3 GB RAM) with windows XP 2009 SP3 operating system. Data were transferred (in ASCII format) for analysis by DATAN package ver. 3.1 [22]. Other calculations were performed in the MATLAB (version 7.8, MathWorks, Inc.) environment. The pH values were measured by a Metrohm 692 model pH-meter equipped with combined Ag/AgCl electrode.

3. Theoretical part

The data for each dye were stored in spectral files as matrices of size n (wavelengths) and m (temperatures) and then processed and analyzed using DATAN [23,24] program.

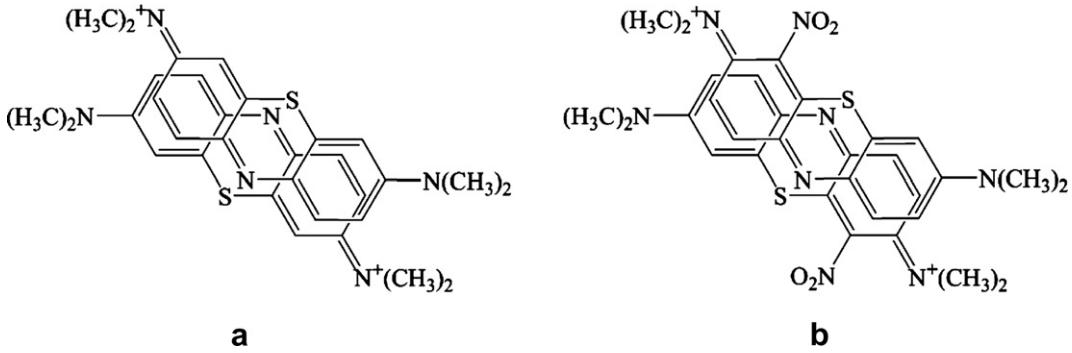

Fig. 2. Probable structures of dimer form of (a) MB and (b) MG. (Only one of four possible resonance configurations is shown).

The absorption spectra recorded at different temperatures are digitized and arranged as rows in a $(n \times m)$ data matrix $\boldsymbol{A}$, where n is the number of data points in each spectrum and m is the number of temperature intervals (in this paper a matrix is denoted as a bold upper case italics e.g. $\boldsymbol{X}$). Matrix $\boldsymbol{A}$ is decomposed into an orthogonal basis set using, for example, NIPALS [25] as;

$$\boldsymbol{A} = TP' + E \approx TP' = \sum_{i=1}^{r} t_i p_i', \tag{1}$$

where t_i $(n \times 1)$ are orthogonal target vectors an p_i' $(1 \times m)$ are orthogonal projection vectors. These are mathematical constructs and do not correspond to any physical property of the system. r is the number of spectroscopically distinguishable components, and E is the error matrix containing experimental noise, if the correct value of r is selected. For a well-designed experiment, E is small compared to TP' and can be discarded.

Assuming a linear response, the recorded spectra are linear combinations of the spectral responses, $v_i(1 \times m)$, of the components:

$$\boldsymbol{A} = CV + E \approx CV = \sum_{i=1}^{r} c_i v_i, \tag{2}$$

where $c_i(n \times 1)$ are vectors containing the component concentrations at the different temperatures. The Eqs. (3) and (4) are related by a rotation matrix $\boldsymbol{R}$:

$$\boldsymbol{C} = T\boldsymbol{R}^{-1}, \tag{3}$$

$$\boldsymbol{V} = \boldsymbol{R}P', \tag{4}$$

where $\boldsymbol{R}$ is $r \times r$ rotation matrix, which for a two-component system has the element:

$$\boldsymbol{R} = \begin{bmatrix} r_{11} & r_{12} \\ r_{21} & r_{22} \end{bmatrix},$$

and therefore,

$$\boldsymbol{R}^{-1} = \frac{1}{r_{11}r_{22} - r_{12}r_{21}} \begin{bmatrix} r_{22} & -r_{12} \\ -r_{21} & r_{11} \end{bmatrix}, \tag{5}$$

Two constraints are used to determine three of the elements in $\boldsymbol{R}$. The first is the spectrum of the monomer, which is measured separately, and the second is the constant total concentration of the dye. Since a single sample is studied, the total concentration must be constant, constraining the matrix $\boldsymbol{R}$ [26]. For monomer–dimer equilibrium, $2X \leftrightarrow X_2$, the total concentration is constant:

$$c_X + 2c_{X_2} = c_{\mathrm{tot}}, \tag{6}$$

Matrix $\boldsymbol{R}$ can now be described by a single scalar r_{21}, and other factors that are determined by the constraints. The value of r_{21} determines the dimer spectrum and the monomer concentration profile. Although any value of r_{21} produces a mathematically acceptable solution, reasonable results, in terms of spectral intensities and non-negative concentrations and spectral responses, are obtained in a relatively narrow range of r_{21} values. Still, the range is, in general, too large for a quantitative analysis. The final constraint, which produces a unique solution, is the thermodynamic relation between temperature and the equilibrium constant. The components' concentrations are related by the law of mass action:

$$K_{\mathrm{D}}(T) = \frac{c_{x_2}(T)/c^{\circ}}{\left(c_x(T)/c^{\circ}\right)^2}, \tag{7}$$

where $c^{\circ} \equiv 1\ \mathrm{mol\ dm^{-3}}$. Assuming that the dimerization constant $K_{\mathrm{D}}(T)$ depends on temperature according to the van't Hoff equation [27]:

$$\frac{\mathrm{d}\ln K_{\mathrm{D}}(T)}{\mathrm{d}(1/T)} = -\Delta H^{\circ}/R, \tag{8}$$

where ΔH° is the molar enthalpy change, $R = 8.31\ \mathrm{J\ mol^{-1}\ K^{-1}}$ is the universal gas constant, and T is the Kelvin temperature. A linear regression of the dimerization constants with respect to $1/T$ is then performed (Eq. (8)), which determines a trial enthalpy change of the reaction. Once a range has been found, r_{21} is varied gradually in this range, and a χ^2 is calculated for each regression of $\ln K_{\mathrm{D}}(T)$ with respect to $1/T$. The r_{21} that produces the best fit determines matrix $\boldsymbol{R}$. The χ^2 is the sum of squared residuals [28] and generally used as a goodness of fit criterion and its value indicate the predictability of the model, i.e. how well the monomer spectrum and r_{21} are determined. The general formula of the χ^2 is:

$$\chi^2 = \sum_{i=1}^{n} \left(A_{\mathrm{exp}} - A_{\mathrm{calc}}\right)^2 / A_{\mathrm{exp}}, \tag{9}$$

where A_{exp} is the expected value and A_{calc} the value calculated from experimental data over n data points.

4. Results and discussion

4.1. Dye aggregation and spectroscopic studies

The electronic absorption spectra of MB, MG and TO, at constant total dye concentrations and different surfactant concentration were recorded over the wavelength range of 500 to 750 nm (for MB and MG) and 350 to 600 nm (for TO) and a temperature range over 15 to 75 °C at 5 °C intervals and pH 7.0. The sample absorption spectra are shown in Fig. 3(1–3a). As it is expected, by increasing the temperature and decreasing the concentration, the monomer form would be predominant over the dimer form. So it is wise to choose the spectrum of the dye at the highest temperature and at lowest concentration as an initial estimate for the monomer in the subsequent calculations. According to Eqs. (1)–(7), the DATAN program commences with a trial value of r_{21}, at a predefined interval, and iterate all of the calculation steps. The iteration stops when all r_{21} values in the preset interval are tested. The K_{D}, dimer spectrum, ΔS and ΔH, correspond to minimum value of the χ^2 statistics, are selected as the final results (according to Eq. (9)).

By increasing temperature the absorption peak for MB, MG and TO appears at around 662 nm, 656 nm and 499 nm, respectively. Also the absorption shoulder around 610 nm, 609 nm, 473 nm decreased for MB, MG and TO, respectively. The sample calculated absorption spectra of the above dyes in monomer and dimer forms are shown in Fig. 3(1–3a, 1–3b). We analyzed the temperature titrations assuming monomer–dimer, monomer–dimer–trimer and even models including higher order aggregates, and found that the monomer–dimer model most adequately describes the data. This suggests equilibrium between just two spectral species, i.e. monomer–dimer equilibrium. The presence of exactly two species is also verified by the isosbestic point at 620 nm, 617 nm, 478 nm for MB, MG and TO respectively.

The optimum concentration was determined in pure water for each dye (Table 1). As can be seen from Table 1, for the two classes of dyes in aqueous solution, the band of highest intensity in dilute solution becomes weaker as the concentration is increased, and new bands appear at other wavelengths. These spectral changes have long been attributed to aggregation of the dye molecules in water to form dimers and higher polymers under the influence of

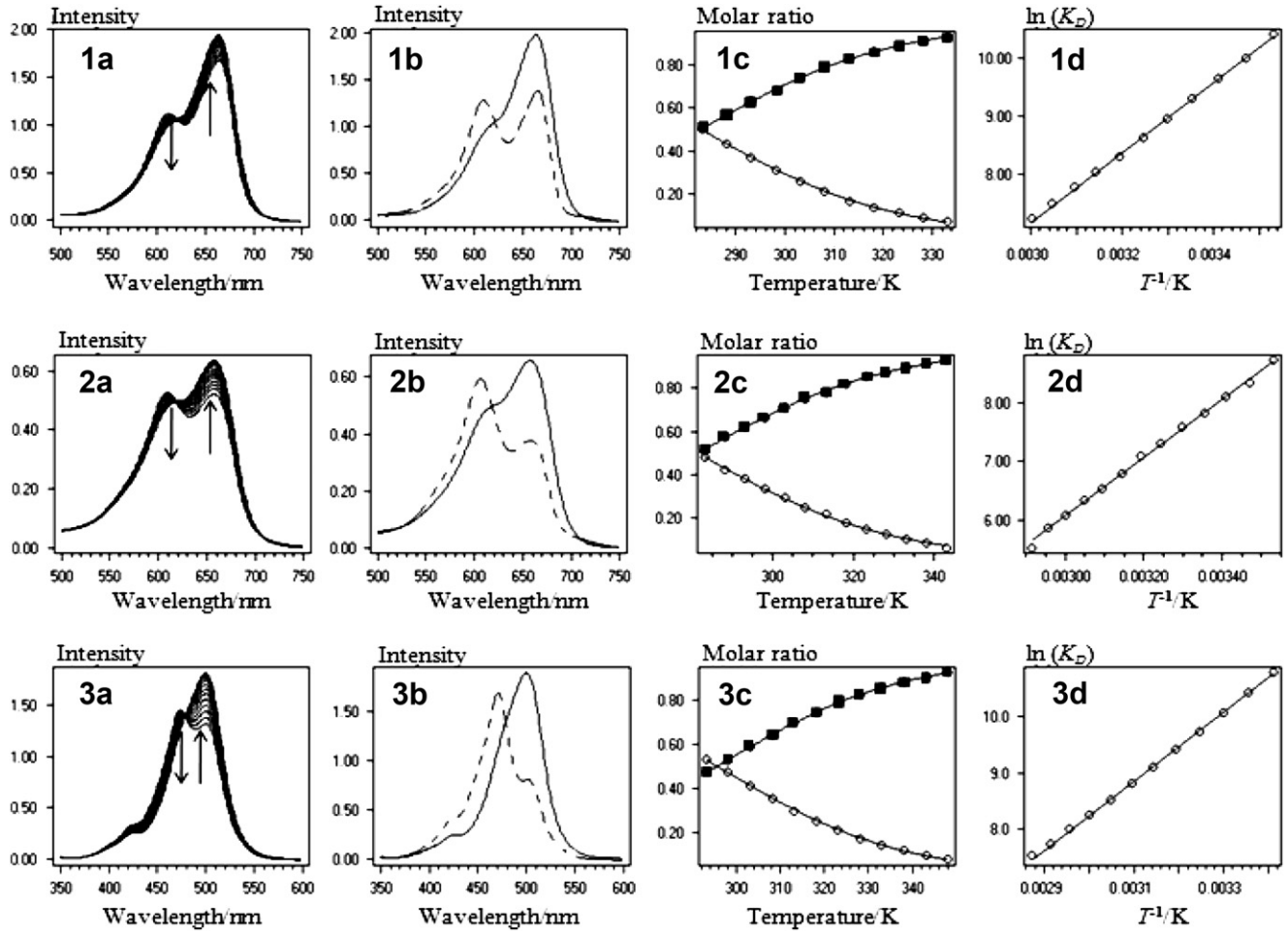

Fig. 3. (a) Absorption spectra, (b) calculated absorption spectra of dimer (- - -) and monomer (—), (c): ■, molar ratio of monomer and ○, molar ratio of dimer, (d) van't Hoff equation plot of (1) MB (3.0×10^{-5} M), (2) MG (1.5×10^{-4} M) and (3) TO (2.5×10^{-5} M) in 5 K intervals between the temperatures 283.15 K and 348.15 K at pH 7.0.

the strong dispersion forces associated with the high polarizability of the chromophoric chain. Also (K_D) was calculated at different temperatures for several total dye concentrations and as expected K_D decreases with increasing temperature while it is virtually independent of total dye concentration. The relative dependence of the dimeric constant of dyes on the various temperatures is shown in Table 2.

From the dependence of log K_D on $1/T$ (Fig. 3(1–3d)), ΔH° and ΔS° values were determined. The dimerization constants at 25 °C and at different concentrations and thermodynamic parameters of the dimerization reactions of the dyes are listed in Table 3. The ΔH° values range from −54.6 to −38.9 kJ mol^{-1} with the mean −46.8 kJ mol^{-1} for MB, and from −60.3 to −31.3 kJ mol^{-1} with the mean −45.8 kJ mol^{-1} for MG and from −58.2 to −40.5 kJ mol^{-1} with the mean −49.4 kJ mol^{-1} for TO. ΔS° ranges from −104 to −56 J mol^{-1} K^{-1} with the mean −80 J mol^{-1} K^{-1}, from −133 to −42 J mol^{-1} K^{-1} with the mean −88 J mol^{-1} K^{-1}, from −109 to −54 J mol^{-1} K^{-1} with the mean −81 J mol^{-1} K^{-1} for MB, MG and TO, respectively. In all cases the dimerization and self association are enthalpy favored and entropy disfavored. As described above, dimerization is presumed to be the dominant form of aggregation in applied concentration ranges in aqueous solutions of MB, MG and TO. This is corroborated by the constancy of the apparent enthalpy of association. In general, the extent of aggregation depends reciprocally on the temperature of the solution and is fully reversible. The observed relationship between entropy and enthalpy reflects an electrostatic nature of the dimerization phenomenon of these three dyes.

4.2. Dye–surfactant interactions and surfactant influence

Surface active agents (surfactants) are amphipathic molecules and they show different properties. Surfactants molecules which also aggregate in solution forming micelles and the concentration

Table 1
Dimeric constant and thermodynamic parameters values of MG and TO at different concentrations in water without surfactant at 25 °C.

Concentration/M	MG			TO				
	1.5×10^{-4}	2.5×10^{-4}	3.5×10^{-4}	2.0×10^{-5}	2.2×10^{-5}	2.5×10^{-5}	2.7×10^{-5}	3.0×10^{-5}
log K_D	3.75	3.44	3.36	4.39	4.43	4.53	4.25	4.11
ΔH/(kJ mol^{-1})	−60.3	−39.3	−38.1	−33.3	−52.8	−51.2	−37.7	−38.1
ΔS/(J mol^{-1} K^{-1})	−130	−66	−63	−28	−92	−85	−45	−49

Table 2
Dimeric constant values of MB, MG and TO dyes at various temperatures.

Temperature/°C	log K_D		
	MB (3.0×10^{-5} M)	MG (1.5×10^{-4} M)	TO (2.5×10^{-5} M)
10	4.52	3.78	
5	4.34	3.62	
20	4.19	3.51	4.68
25	4.04	3.40	4.53
30	3.89	3.29	4.38
35	3.75	3.17	4.23
40	3.60	3.08	4.09
45	3.49	2.95	3.95
50	3.37	2.83	3.82
55	3.25	2.75	3.70
60	3.14	2.64	3.58
65		2.54	3.47
70		2.40	3.36
75			3.26

at which micelles form is known as the critical micelle concentration (CMC). The molecular structures and CMC of the surfactants used in this study are shown in Table 4. The CMC is the most important characteristic of a surfactant and is useful for consideration of the practical applications of surfactants.

The physical properties of surfactants differ from those of smaller or nonamphipathic molecules in one major aspect, namely the abrupt changes in their properties above a critical concentration [29]. At low concentrations, most properties are similar to those of a simple electrolyte. At the CMC or above strongly cooperative binding is indicated and there is an onset association of surfactant with the dye molecules. At this concentration (i.e. at CMC concentration), the molecules of dye saturated with micelle. An added surfactant will interact strongly with the hydrophobic groups of the dye molecules, leading to a strengthened association between the surfactant molecules and the dye molecules (Fig. 4).

Initially the surfactant monomers interact with the hydrophobic groups of the dye molecules, and act as a physical cross linker between them to facilitate the creation of dimer form and result in maximum dimerization. At higher surfactant concentrations, the micelles, which are now abundant, will no longer be shared between the molecules of dye, i.e. they lost their cross-linker role. This effect can be observed of the visible absorption spectra of MB, MG and TO with fixed concentration (1.85×10^{-4}, 2.12×10^{-4} and 2.89×10^{-4} M respectively) in aqueous solution of the surfactant having different chemical structures, above CMC, which are shown in Fig. 5. The spectral data obtained in aqueous surfactant solutions

Table 4
The molecular structures and CMC of cationic and natural surfactants.

Surfactant	CMC/mM	Type of surfactant	Molecular structure
HTAB	0.92	Cationic	$CH_3(CH_2)_{15}N(Br)(CH_3)_3$
Triton X-100	0.22	Neutral	t-Oct-C_6H_4-$(OCH_2CH_2)_x$OH, $x = 9–10$
Triton X-114	0.20	Neutral	$(C_2H_4O)n$ $C_{14}H_{22}O$, $n = 7$ or 8

were compared to those obtained in water. The visible spectra presented in Fig. 5 clearly show that the dye–surfactant interactions, above the CMC, result in a clear reduction in the shoulder intensity of the absorption spectra of three dyes and the profound effect in the case of TO, indicating the elimination or reduction of the dye aggregates in the micelle environment.

Previous study has shown that the highest value of the viscosity of the surfactant at CMC concentration can also boost the dimer formation [30].

4.3. Effect of ionic strengths and organic solvents

For studying the effect of ionic strength on the dimerization of the dyes, three different concentrations of potassium chloride (from 0.50, 1.00 and 1.50 M), were selected and dimerization was investigated. To maintain a constant pH of the solutions', a neutral buffer solution was chosen (the concentrations of buffer constituents are negligible with respect to the inert salts as supporting electrolytes). A preliminary study showed that, application of the neutral to basic buffer solutions, the three dyes show just a very minor change in their spectral patterns (i.e. the changing of the pH of the solutions has no observable effect on the spectral behavior of the dye solutions). Also, according to findings of Mchedlov–Petrosyan et al. [31] the dominant monomer species around this pH (7.50) is a zwitterion, which bears positive and negative charge simultaneously and has a tautomeric isomer with zero charge especially in some nonaqueous solutions. Hydrogen bonding, hydrophobic forces, and electrostatic interactions are all considered important for the dimerization. What effect we expected from increasing the ionic strength on the dimerization constants according to extended Debye–Huckel equation [32], is totally depend on the relative change in the total charge of the dimer species with respect to the two monomer moieties. As it can be seen from the data obtained at different ionic strength (Table 5), the increase of the ionic strength results in a decrease of the dimerization constants. The dimeric constants at 25 °C and

Table 3
Dimeric constant (K_D) and thermodynamic values of MB, MG and TO dyes at various concentration of surfactants at 25 °C.

Concentration/mM	HTAB			Triton X-100			Triton X-114		
	0.25	0.92 (CMC)	2.00	0.05	0.22 (CMC)	0.30	0.05	0.20 (CMC)	0.30
Thiazole orange (2.5×10^{-5} M)									
$\Delta H°$/(kJ mol^{-1})	−40.5	−49.4	−51.1	−45.2	−58.2	−50.3	−41.4	−56.2	−52.1
$\Delta S°$/(J mol^{-1} K^{-1})	−54	−82	−89	−68	−109	−84	−59	−101	−90
log K_D	4.25	4.34	4.16	4.33	4.50	4.40	4.18	4.53	4.42
Methylene green (1.5×10^{-4} M)									
$\Delta H°$/(kJ mol^{-1})	−31.2	−41.5	−42.0	−45.8	−44.5	−40.8	−59.6	−42.9	−43.0
$\Delta S°$/(J mol^{-1} K^{-1})	−42	−72	−75	−87	−81	−74	−133	−75	−81
log K_D	3.24	3.49	3.41	3.47	3.56	3.25	3.46	3.58	3.27
Methylene blue (3.0×10^{-5} M)									
$\Delta H°$/(kJ mol^{-1})	−39.0	−39.4	−38.9	−48.4	−54.6	−47.9	−39.1	−52.5	−40.2
$\Delta S°$/(J mol^{-1} K^{-1})	−58	−57	−58	−88	−104	−85	−56	−99	−62
log K_D	3.81	3.9	3.77	3.86	4.09	3.92	3.89	3.99	3.79

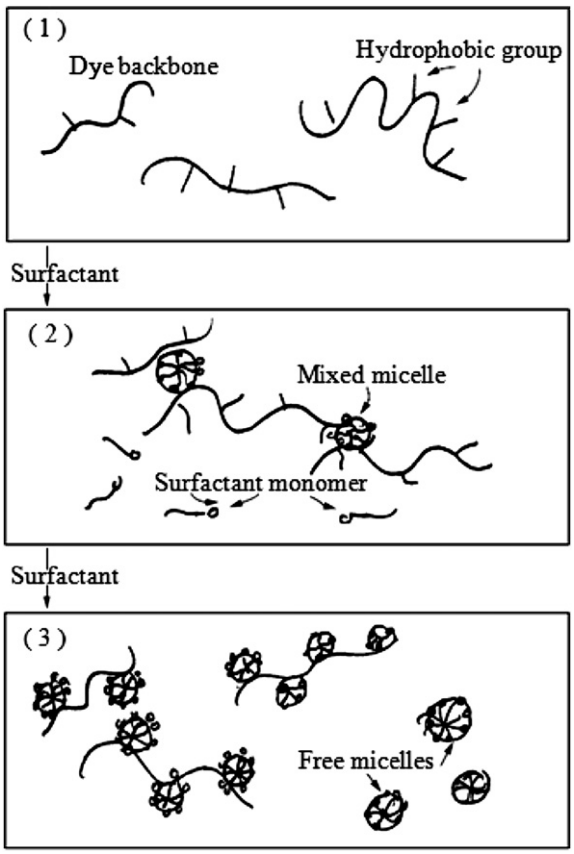

Fig. 4. Interaction between surfactant and dimer form of dye.

thermodynamic parameters values of MB, MG and TO at different ionic strengths of potassium chloride are listed in Table 5 and they are compared with previously reported data [33,34].

One of the most interesting points of changing the ionic strength on the dimerization reactions of the three dyes is the spectral change of the dimer form. The dimer spectra of MB, MG and TO show enhancement of the intensity of the spectral band with λ_{max}'s around 622 nm, 656 nm and 499 nm for MB, MG and TO respectively as compared with those in water. Patil et al. [35] reported a similar spectral change from the effect of the addition of some solutes to the aqueous solution of methylene blue. They additionally showed that these spectral variations depend upon the angle between the planes of the two dye molecules which in turn depend upon the concentration of the inert solutes. The decrease in K_D values with increase in the concentration of each of the inert salts also indicates the decreasing tendency of the dyes molecules to undergo aggregation. The random variations in the formation constants by changing ionic strengths (Table 5) may indicate a return to the presence of the some unaccounted for interactions such as cation–anion (dye-Cl^-) attractive type interactions, in addition to monomer–dimer equilibrium.

In order to study the effect of organic solvents on the dimerization constants for these three dyes, various binary dioxane–water and methanol–water mixtures have been examined. These water–miscible additives shift the monomer–dimer equilibrium of the dyes in the direction of the monomer. The dominant role of water as the most favorable solvent to aggregation of ionic dyes is no doubt associated with the effect of its high dielectric constant in reducing the repulsive force between the similarly charged dye cations or anions in the aggregate. Lack of such an effect in nonpolar solvents with a low dielectric constant excludes the dimerization of

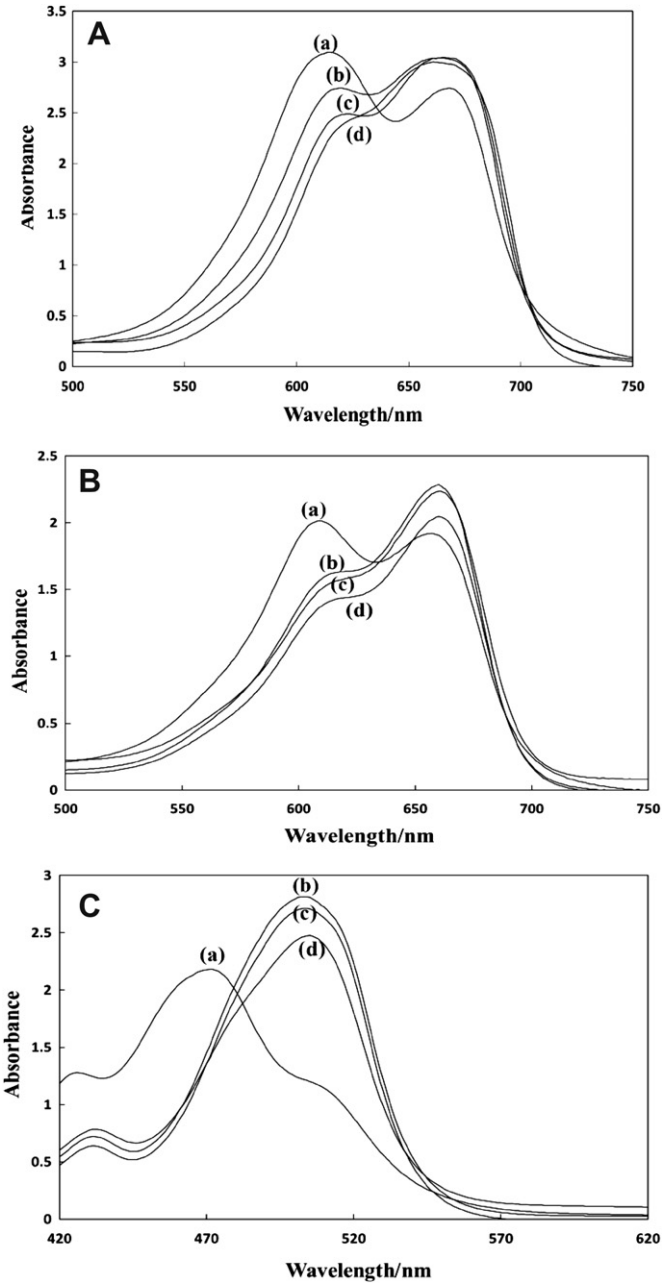

Fig. 5. The effect of different surfactants on the aggregation of the dyes after CMC concentrations. (a) free dye (b) Triton X-100 (c) Triton-X 114 (d) HTAB for MB, MG and TO in A, B and C respectively.

the ionic dyes. But the absence of aggregation in organic solvents of high dielectric constants and low solvating ability in comparison to the water suggests that solvation interferes with the aggregation, and in such solvents aggregates are stable only at low temperatures and under high viscosity [36].

4.4. Type of aggregation

Dyes are well known to aggregate in aqueous solution. The π stacking of the conjugated systems of the dyes is favored based on both the hydrophobicity and polarizability of the dye. To date, the best description of the aggregation behavior of dye chromophores is based on the exciton-splitting theory [37]. The relative intensity

Table 5
Compare of dimeric constant (K_D) and thermodynamic values of MB, MG and TO with previous reported data, at various concentration of salt and different ionic strengths at 25 °C.

	Our study				Previous reports			
MB								
Dye Conc./M	3.0×10^{-5}	3.0×10^{-5}	3.0×10^{-5}	3.0×10^{-5}	6.0×10^{-5}	5.0×10^{-5}	5.0×10^{-5}	5.0×10^{-5}
NaCl Conc./M	–	–	–	–	–	–	–	–
KCl Conc./M	–	0.5	1.0	1.5	–	0.5	1.0	1.5
ΔH°/(kJ mol^{-1})	−50.3	−45.8	−53.7	−60.1	−49.2	−63.4	−63.6	−62.0
ΔS°/(J mol^{-1} K^{-1})	−91	−74	−94	−113	−82	−117	−116	−107
log K_D	4.04	4.14	4.48	4.63	4.31	5.09	5.15	5.33
MG								
Dye Conc./M	1.5×10^{-4}	1.5×10^{-4}	1.5×10^{-4}	1.5×10^{-4}	1.54×10^{-4}	1.54×10^{-4}	1.54×10^{-4}	1.54×10^{-4}
NaCl Conc./M	–	–	–	–	–	0.6	0.9	1.5
KCl Conc./M	–	0.5	1.5	1.5	–	–	–	–
ΔH°/(kJ mol^{-1})	−60.3	−33.1	−48.9	−56.9	−74.9	−52.6	−41.3	−35.2
ΔS°/(J mol^{-1} K^{-1})	−130	−38	−93	−112	−141	−96	−63	−93
log K_D	3.75	3.83	3.72	4.12	4.39	4.23	3.92	4.25
TO								
Dye Conc./M	2.5×10^{-5}	2.5×10^{-5}	2.5×10^{-5}	2.5×10^{-5}	–	–	–	–
NaCl Conc./M	–	–	–	–	–	–	–	–
KCl Conc./M	–	0.5	1.5	1.5	–	–	–	–
ΔH°/(kJ mol^{-1})	−51.2	−49.4	−53.9	−52.7	–	–	–	–
ΔS°/(J mol^{-1} K^{-1})	−85	−77	−90	−87	–	–	–	–
log K_D	4.53	4.63	4.75	4.69	–	–	–	–

of the absorption bands can provide structural information about the dimer regarding its simplest geometry model (e.g., the chromophore spacing and the relative spatial arrangement of the transition dipole moments of the molecules forming the dimers). The self-association of dyes in solution or at the solid-liquid interface is a frequently encountered phenomenon in dye chemistry owing to strong intermolecular van der Waals-like attractive forces between the molecules. The aggregates in solution exhibit distinct changes in the absorption band as compared to the monomeric species. From the spectral shifts, various aggregation patterns of the dyes in different media have been proposed. Two limiting types of supramolecular structures are formed and are referred to as "H" and "J" aggregates. The processes of conversion of the monomer into the J-aggregate upon thermal initiation and to the H-aggregate

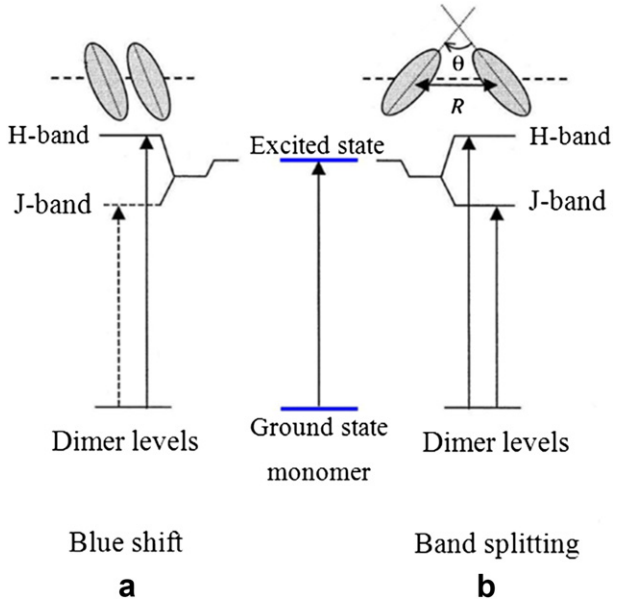

Fig. 6. Exciton band energy diagram for molecular dimmers in (a) a parallel plane twist angle configuration and in (b) an oblique in-plane configuration.

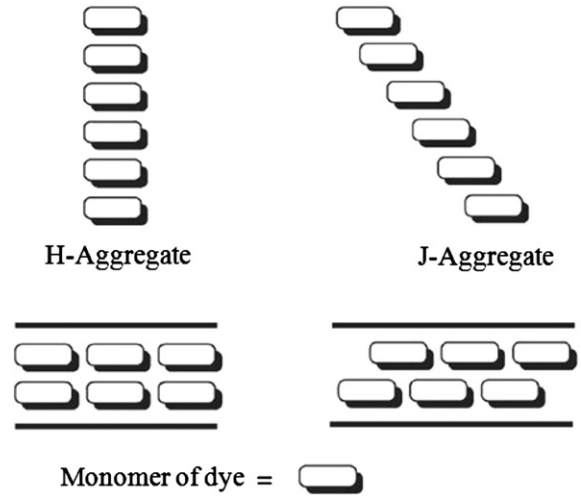

Fig. 7. Illustration of H- and J-aggregation by dye molecule in water.

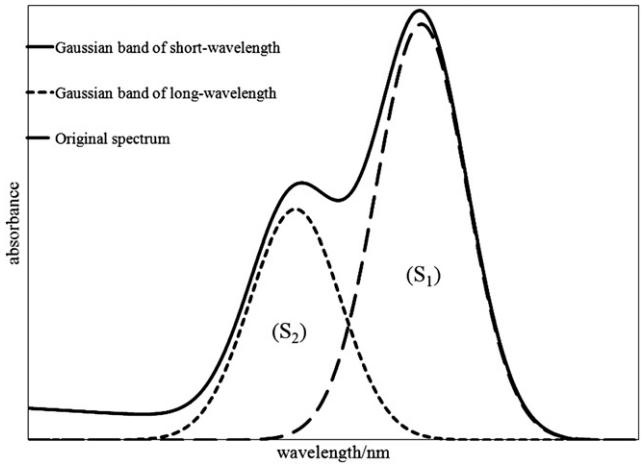

Fig. 8. Schematic spectrum decomposition into Gaussian shapes.

Table 6
Excitonic parameters of dye aggregates at various temperatures.

Temperature/°C	10	15	20	25	30	35	40	45	50	55	60
Methylene blue (3.0×10^{-5} M)											
θ/°	−0.92	−0.99	−1.04	−1.09	−1.12	−1.14	−1.16	−1.19	−1.19	−1.20	−1.20
$\lambda_{shoulder}$/nm	612	613	613	614	614	616	616	617	617	617	618
λ_{max}/nm	664	665	664	664	664	664	664	664	664	664	664
$A_{shoulder}$	1.09	1.06	1.04	1.03	1.02	1.02	1.01	1.00	1.00	1.00	1.00
A_{max}	1.66	1.70	1.74	1.78	1.82	1.84	1.87	1.90	1.91	1.92	1.93
$A_{shoulder}/A_{max}$	0.65	0.62	0.60	0.58	0.56	0.55	0.54	0.53	0.52	0.52	0.52
U/cm^{-1}	639.81	637.81	626.49	613.20	613.20	586.76	586.76	573.61	573.61	573.61	560.49

Temperature/°C	10	15	20	25	30	35	40	45	50	55
Methylene green (1.5×10^{-4} M)										
θ/°	−0.03	−0.12	−0.20	−0.27	−0.34	−0.40	−0.46	−0.52	−0.56	−0.59
$\lambda_{shoulder}$/nm	609	610	611	611	612	613	613	615	616	617
λ_{max}/nm	658	658	658	658	658	658	658	658	658	658
$A_{shoulder}$	0.49	0.48	0.48	0.48	0.47	0.47	0.47	0.47	0.46	0.46
A_{max}	0.49	0.51	0.53	0.54	0.55	0.56	0.57	0.58	0.59	0.60
$A_{shoulder}/A_{max}$	0.99	0.94	0.91	0.89	0.86	0.84	0.82	0.80	0.78	0.77
U/cm^{-1}	611.40	597.94	584.52	584.52	571.15	557.82	557.82	531.30	518.10	504.94

Temperature/°C	20	25	30	35	40
Thiazole orange (2.5×10^{-5} M)					
θ/°	0.16	0.07	−0.04	−0.16	−0.25
$\lambda_{shoulder}$/nm	474	474	475	477	479
λ_{max}/nm	500	500	500	500	500
$A_{shoulder}$	1.43	1.42	1.40	1.38	1.06
A_{max}	1.31	1.37	1.43	1.48	1.54
$A_{shoulder}/A_{max}$	1.09	1.03	0.98	0.93	0.68
U/cm^{-1}	548.52	548.52	526.32	482.18	438.41

upon photoexcitation are schematically shown in Fig. 6. The J- and H-aggregates of dyes differ from one another in the relative position of molecules and their number. Dye molecules in dimers and H-aggregates are packed into a sandwich structure, whereas the molecules in J- aggregates are packed 'following a brickwork pattern, which imparts very different spectral properties to these species (Fig. 7) [38]. The aggregation of a dye leads to a strong coupling of the molecular transition dipoles, i.e. the electrostatic interaction between molecular transition dipoles of the chromophores causes the splitting of energy levels of the excited states of the molecules, while the ground state of the dimer remains doubly degenerate. According to Kasha exciton theory [39], J- or H-aggregates can be formed depending on the angle between the transition dipoles and the molecular axis of the aggregate. For H-aggregates, the chromophores of the participating molecules are in parallel two planes, while in J-aggregate (linear structure) they are in the same plane. However, real dye systems tend to form both Hand J-aggregates.

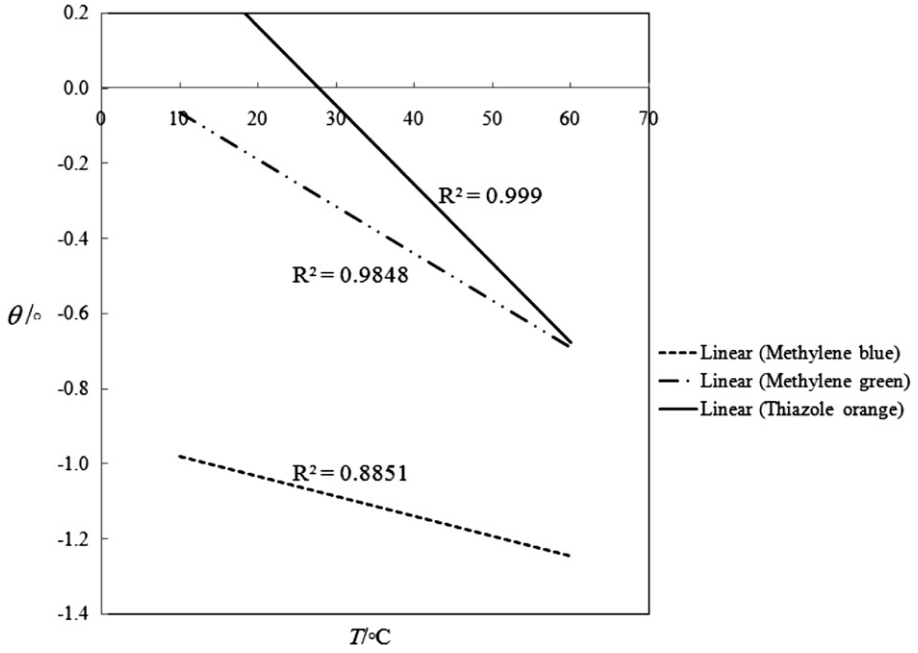

Fig. 9. The angle existing between the monomer units versus temperature for MB, MG and TO.

The angle between the chromophores was obtained with the following considerations. As can be seen from Fig. 8, the intense band with a Gaussian shape was centered at the maximum of the spectrum. The second Gaussian band was obtained by subtracting the first band from the total visible spectrum. Assuming that the distance between the dipoles remains unchanged, the angle existing between the monomer units, θ, in the dimer was determined from the ratio between the areas of the long-wavelength (S_1) and the short-wavelength (S_2) of the two Gaussian bands, $\tan^2(\theta/2) = S_1/S_2$ [40]. The difference in the energy of the split-levels depends on the interaction energy (U), between the dye molecules in the dimer species. The interaction energy can be obtained by considering the half of the frequency difference existing between the maximum of the neighboring bands: $U/\mathrm{cm}^{-1} = (1/2)(\bar{\nu}_{\mathrm{shoulder}} - \bar{\nu}_{\mathrm{max}})$.

One of the most factors which determine the type of aggregation is substituents on the hydrophobic rings of the dye molecules. Unsubstituted dyes generally favor H-aggregation as this provides the greatest number of van der Waals interactions and minimizes exposure to water. However, substituents placed at various positions on the dye structure can promote J-aggregation due to steric and/or electrostatic factors. H- and J-aggregates typically exhibit absorption maxima that are shifted to either shorter or longer wavelength, respectively (Table 6). Future increase of temperature was observed to promote the conversion from H dimers to J-dimers. The conversion from H- to J-aggregates, caused a decrease of interaction energy (U) (Figs. 9 and 10). It is known that short-wavelength absorption bands can correspond to H-aggregates. On this basis, we assume that the short-wavelength band observed in our experiments belongs to H-aggregates formed upon the photo-initiated transformation of the monomer form. The bathochromically shifted J-bands and hypsochromically shifted H-bands of the aggregates have been explained in terms of molecular exciton coupling theory, i.e., coupling of transition moments of the constituent dye molecules.

We also study on the exitonic parameters of pure MB, MG and TO at different concentrations in water were studied (Table 7) and the effect of surfactants on their parameters were also explored (Table 8). The results in Table 8 showed that the angle existing between the monomer units (θ), in the dimer and interaction energy (U), between the dye molecules in the dimer species, was not dependent on the interaction of dyes with surfactant molecules at various concentration (especially pre- and post-micellar regimes). The columbic interaction and steric hindrance of the dyes with surfactant molecules formed dye–surfactant aggregate structures. Dye interaction and aggregation in surfactant solutions can be explained by Kasha excitonic theory as discussed above, in pre- and post-micellar regimes. Furthermore, we observed that the concentration of surfactant (below CMC, at CMC and a concentration higher than CMC) have an effect on dimerization constant (K_D) and does not have an enormous effect on aggregate formation and interaction energy between the two monomer units in the dimer structure. We may suppose that the formation of J-aggregates requires significant movement inside a dispersion

Table 7
Excitonic parameters of dye aggregates at various dye concentrations at 25 °C.

Thiazole orange					
Concentration/M	2.0E−5	2.2E−5	2.5E−5	2.7E−5	3.0E−5
θ/°	−0.03	0.02	0.07	0.11	0.17
$\lambda_{\mathrm{shoulder}}$/nm	475	475	474	474	474
λ_{max}/nm	500	500	500	500	500
A_{shoulder}	1.18	1.31	1.42	1.65	1.76
A_{max}	1.20	1.30	1.37	1.55	1.61
$A_{\mathrm{shoulder}}/A_{\mathrm{max}}$	0.99	1.01	1.03	1.06	1.10
U/cm^{-1}	526.32	526.32	548.52	548.52	548.52
Methylene green					
Concentration/M	1.5E−4		2.5E−4		3.5E−4
θ/°	−0.27		−0.04		0.09
$\lambda_{\mathrm{shoulder}}$/nm	611		610		609
λ_{max}/nm	658		658		658
A_{shoulder}	0.48		0.82		1.12
A_{max}	0.54		0.83		1.07
$A_{\mathrm{shoulder}}/A_{\mathrm{max}}$	0.89		0.98		1.05
U/cm^{-1}	572.96		597.94		611.40

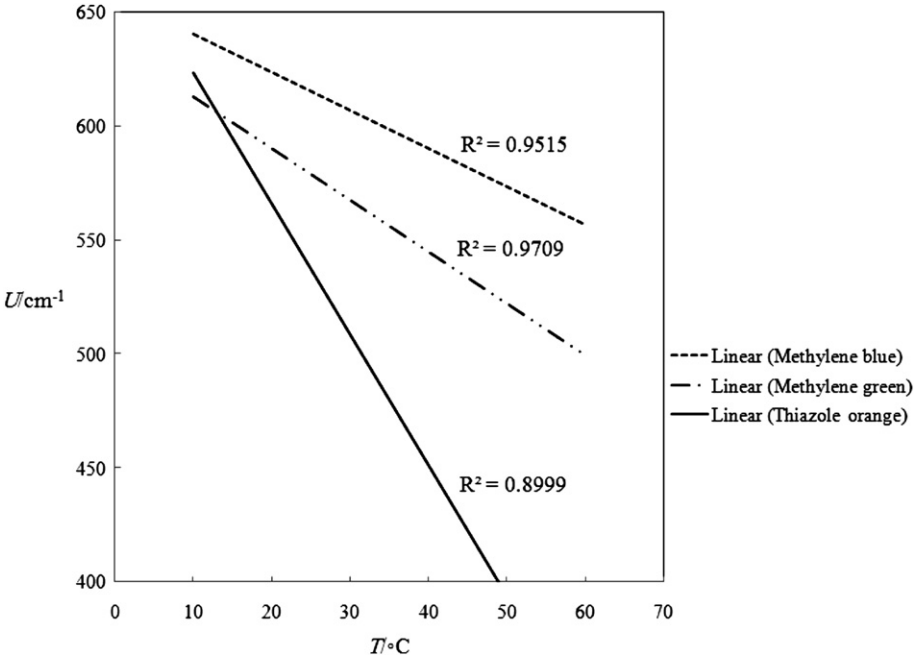

Fig. 10. Decrease of interaction energy versus increase of temperature for MB, MG and TO.

Table 8
Excitonic parameters of dye aggregates at various surfactant concentrations at 25 °C.

Concentration	Free dye	T-X100			T-X114			HTAB		
	3.0×10^{-5} M	0.05 mM	0.22 mM	0.30 mM	0.05 mM	0.20 mM	0.30 mM	0.25 mM	0.92 mM	2.00 mM
Methylene blue (3.0×10^{-5} M)										
$\theta/^\circ$	−1.09	−1.12	−1.11	−1.09	−1.11	−1.16	−1.14	−0.98	−0.99	−1.00
$\lambda_{shoulder}$/nm	614	615	615	615	615	616	616	614	613	614
λ_{max}/nm	664	664	664	664	664	665	665	664	664	664
$A_{shoulder}$	1.03	0.91	1.00	0.94	0.92	0.70	0.78	1.32	1.37	1.31
A_{max}	1.78	1.61	1.75	1.65	1.61	1.29	1.41	2.11	2.18	2.11
$A_{shoulder}/A_{max}$	0.58	0.56	0.57	0.57	0.57	0.54	0.55	0.63	0.63	0.62
U/cm^{-1}	613.20	599.96	599.96	599.96	599.96	598.09	598.09	613.20	626.49	613.20
Methylene green (1.5×10^{-4} M)										
	1.5×10^{-4} M	0.05 mM	0.22 mM	0.30 mM	0.05 mM	0.20 mM	0.30 mM	0.25 mM	0.92 mM	2.00 mM
$\theta/^\circ$	−0.27	−0.28	−0.29	−0.29	−0.29	−0.29	−0.29	−0.27	−0.26	−0.26
$\lambda_{shoulder}$/nm	611	611	611	612	612	612	612	611	611	611
λ_{max}/nm	658	658	658	658	658	658	658	658	658	658
$A_{shoulder}$	0.48	0.47	0.47	0.47	0.47	0.46	0.47	0.48	0.48	0.48
A_{max}	0.54	0.53	0.54	0.53	0.54	0.53	0.53	0.54	0.54	0.54
$A_{shoulder}/A_{max}$	0.89	0.88	0.88	0.88	0.88	0.88	0.88	0.88	0.89	0.89
U/cm^{-1}	572.96	572.96	572.96	571.15	571.15	571.15	571.15	572.96	572.96	572.96
Thiazole orange (2.5×10^{-5} M)										
	2.5×10^{-5} M	0.05 mM	0.22 mM	0.30 mM	0.05 mM	0.20 mM	0.30 mM	0.25 mM	0.92 mM	2.00 mM
$\theta/^\circ$	0.07	0.05	−0.01	−0.01	−0.08	−0.11	−0.14	−0.04	−0.05	−0.06
$\lambda_{shoulder}$/nm	474	475	475	475	476	476	476	475	475	476
λ_{max}/nm	500	500	500	500	500	500	500	500	500	500
$A_{shoulder}$	1.42	1.37	1.24	1.31	1.11	1.05	1.06	1.18	1.17	1.13
A_{max}	1.37	1.34	1.25	1.32	1.15	1.11	1.13	1.20	1.19	1.16
$A_{shoulder}/A_{max}$	1.03	1.02	0.99	0.99	0.96	0.95	0.94	0.98	0.98	0.97
U/cm^{-1}	548.52	526.32	526.32	526.32	504.20	504.20	504.20	526.32	526.32	504.20

particle, whereas insignificant displacement of molecules from one another is sufficient to form the dimer (and, possibly, an H-aggregate). If it were possible to selectively vary the mobility of molecules during heating or photoexcitation, the problem of the formation of aggregates with preset composition and properties would be solved.

5. Conclusion

The molecular association of ionic dyes in solutions is due to the strongly attractive electrostatic forces. The strength of the molecular association depends on the several factors including the dye concentration, temperature, solvent and other factors. The thermodynamic parameters, enthalpy and entropy of the dimerization reaction were calculated from the dependence of dimeric constant on the temperature (van't Hoff equation). The interaction between dye molecules is attributed predominantly to enthalpic rather than entropic reasons. The dimerization forces between the dye molecules are dispersive van der Waals interactions and K_D depends on the size and rigidity of the dye molecules and also viscosity of surfactant at different concentration. The structures of the aggregates were studied by applying exciton theory to the analysis of the absorption spectra. The application of the exciton theory to the H-dimers and J-dimers has allowed the determination of the spatial arrangement of the molecules (e.g., in-plane oblique angle configuration) and the structural parameters that define such an arrangement (θ and U).

Acknowledgements

Our sincere thanks to all the people who have contributed to and worked on this manuscript. We would like to express our sincere gratitude to our friends at analytical laboratory of Razi University and chemometrics laboratory of K. N. Toosi University of Technology.

References

[1] Taguchi T, Hirayama S, Okamoto M. New spectroscopic evidence for molecular aggregates of rhodamine 6G in aqueous solution at high pressure. Chemical Physics Letters 1994;231:561–8.
[2] Roderich R. Ullmann's encyclopedia of industrial chemistry. 6th ed. Leverkusen-Federal Republic of Germany: Wiley-Vch Bayer AG; 2003. pp. 293–14.
[3] Yang R, Ruan C, Deng J. A H_2O_2 biosensor based on immobilization of horseradish peroxidase in electropolymerized methylene green film on GCE. Journal of Applied Electrochemistry 1998;28:1269.
[4] Raue R. Azine dyes. Ullmann's encyclopedia of industrial chemistry; 2000.
[5] Impert O, Katafias A, Kita P, Mills A, Pietkiewicz-Graczyk A, Wrzeszcz G. Kinetics and mechanism of a fast leuco-Methylene Blue oxidation by copper(II)–halide species in acidic aqueous media. Journal of the Chemical Society Dalton Transactions; 2003:348–53.
[6] Tognalli N, Fainstein A, Vericat C, Vela M, Salvarezza R. In situ raman spectroscopy of redox species confined in self-assembled molecular films. Journal of Physical Chemistry B 2008;112:3741–6.
[7] Dilgin Y, Nisli G. Fluorimetric determination of ascorbic acid in vitamin C tablets using methylene blue. Chemical & Pharmaceutical Bulletin 2005;53:1251–4.
[8] Adamcikova L, Pavlikova K, Sevcik P. The methylene blue-D-glucose-O_2 system. Oxidation of D-glucose by methylene blue in the presence and the absence of oxygen. International Journal of Chemical Kinetics 1999;31:463–8.
[9] Fujita K, Taniguchi K, Ohno H. Dynamic analysis of aggregation of methylene blue with polarized optical waveguide spectroscopy. Talanta 2005;65:1066–70.
[10] Armitage BA. Cyanine dye–nucleic acid interactions. Berlin Heidelberg: Springer-Verlag; 2008. p. 17.
[11] Armitage BA. Cyanine dye–DNA interactions: intercalation, groove binding, and aggregation. Berlin Heidelberg: Springer-Verlag; 2005.
[12] Ghasemi J, Niazi A, Westman G, Kubista M. Thermodynamic characterization of the dimerization equilibrium of an asymmetric dye by spectral titration and chemometric analysis. Talanta 2004;62:835–41.
[13] Nygren J, Andrade JM, Kubista M. Characterization of a single sample by combining thermodynamic and spectroscopic information in spectral analysis. Analytical Chemistry 1996;68:1706–10.
[14] Jafari A, Ghanadzadeh A, Tajalli H, Yeganeh M, Moghadam M. Electronic absorption spectra of cresyl violet acetate in anisotropic and isotropic solvents. Spectrochimica Acta Part A 2007;66:717–25.
[15] Ghasemi J, Niazi A, Kubista M. Thermodynamics study of the dimerization equilibria of rhodamine B and 6G in different ionic strengths by photometric titration and chemometrics method. Spectrochimica Acta Part A 2005;62:649–56.
[16] Dakiky M, Nemcova I. Aggregation of o, o′-dihydroxyazo dyes-1. Concentration, temperature, and solvent effect. Dyes and Pigments 1999;40:141–50.
[17] Green FJ. Dyes and indicators. Milwaukee: The Sigma–Aldrich handbook of stains; 1991.

[18] Miljanic S, Cimerman Z, Frkanec L, Zinic M. Lipophilic derivative of rhodamine 19: characterization and spectroscopic properties. Analytica Chimica Acta 2002;468:13–25.
[19] Ghanadzadeh A, Tajalli H, Zirack P, Shirdel J. On the photo-physical behavior and electro-optical effect of oxazine dyes in anisotropic host. Spectrochimica Acta Part A 2004;60:2925–32.
[20] Ghanadzadeh A, Zeini A, Kashef A, Moghadam M. Concentration effect on the absorption spectra of oxazine1 and methylene blue in aqueous and alcoholic solutions. Journal of Molecular Liquids 2008;138:100–6.
[21] Tafulo PAR, Queirós RB, González-Aguilar G. On the "concentration-driven" methylene blue dimerization. Spectrochimica Acta Part A 2009;73:295–300.
[22] http://www.multid.se.
[23] Scarmino I, Kubista M. Analysis of correlated spectral data. Analytical Chemistry 1993;65:409–16.
[24] Ghasemi J, Niazi A, Kubista M, Elbergali A. Spectrophotometric determination of acidity constants of 4-(2-pyridylazo)resorcinol in binary methanol–water mixtures. Analytica Chimica Acta 2002;455:335–42.
[25] Kubista M, Sjoback R, Nygren J. Quantitative spectral analysis of multicomponent equilibria. Analytica Chimica Acta 1995;302:121–5.
[26] Eriksson S, Kim SK, Kubista M, Norden B. Binding of 4′6-diamidino-2-phenylindole (DAPI) to AT regions of DNA: evidence for an allosteric conformational change. Biochemistry 1993;32:2987–98.
[27] Levine LV. Physical chemistry. New York: McGraw-Hill; 1988.
[28] Kubista M, Nygren J, Elbergali A, Sjoback R. Making reference samples redundant. Critical Reviews in Analytical Chemistry 1999;29:1–28.
[29] Holmberg K, Jonsson B, Kronberg B, Lindman B. Surfactants and polymers in aqueous solution. Germany: John Wiley & Sons; 2003. pp. 41–4.
[30] Tadros TF. Applied surfactants principles and applications. Germany: John Wiley & Sons; 2005. pp. 45–8.
[31] Peterson OG, Tuccio SA, Snavely BB. CW operation of an organic dye solution LASER. Applied Physics Letters 1970;17:245–8.
[32] Debye P, Hückel E. On the theory of electrolytes. I. freezing point depression and related phenomena. Physikalische Zeitschrift 1923;24:185–206.
[33] Ghasemi J, Lotfi SH, Mazloum Ardaki M, Noroozi M. Thermodynamics study of the dimerization equilibria of methylene green in different ionic strengths by photometric titration and chemometric method. Analytical Chemistry An Indian Journal 2006;2:216–23.
[34] Ghasemi J, Miladi M. Association equilibrium of methylene blue by spectral titration and chemometrics analysis: a thermodynamic study. Journal of the Chinese Chemical Society 2009;56:459–68.
[35] West W, Pearce S. The dimeric state of cyanine dyes. Journal of Physical Chemistry 1965;69:1894–903.
[36] Patil K, Pawar R, Talap P. Self-aggregation of methylene blue in aqueous medium and aqueous solutions of Bu_4NBr and urea. Physical Chemistry Chemical Physics 2000;2:4313–7.
[37] McRae EG, Kasha M. Physical processes in radiation biology. 1st ed. New York: Academic Press; 1964.
[38] Czikkely V, Forsterling H, Kuhn H. Light absorption and structure of aggregates of dye molecules. Chemical Physics Letters 1970;6:11–4.
[39] Kasha M, Rawls HR, El-Bayoumi MA. The exciton model in molecular spectroscopy. Pure and Applied Chemistry 1965;1:371–92.
[40] Ferrer ML, Del Monte F, Levy D. Rhodamine 19 fluorescent dimers resulting from dye aggregation on the porous surface of sol–gel silica glasses. Langmuir 2003;19:2782–6.